J Comput Aided Mol Des (2012) 26:947–961
DOI 10.1007/s10822-012-9585-7

Structural prediction of a novel chitinase from the psychrophilic *Glaciozyma antarctica* PI12 and an analysis of its structural properties and function

Aizi Nor Mazila Ramli · Nor Muhammad Mahadi · Mohd Shahir Shamsir · Amir Rabu · Kwee Hong Joyce-Tan · Abdul Munir Abdul Murad · Rosli Md. Illias

Received: 18 November 2011 / Accepted: 4 June 2012 / Published online: 19 June 2012

Abstract The structure of psychrophilic chitinase (CHI II) from *Glaciozyma antarctica* PI12 has yet to be studied in detail. Due to its low sequence identity (<30 %), the structural prediction of CHI II is a challenge. A 3D model of CHI II was built by first using a threading approach to search for a suitable template and to generate an optimum target-template alignment, followed by model building using MODELLER9v7. Analysis of the catalytic insertion domain structure in CHI II revealed an increase in the number of aromatic residues and longer loops compared to mesophilic and thermophilic chitinases. A molecular dynamics simulation was used to examine the stability of the CHI II structure at 273, 288 and 300 K. Structural analysis of the substrate-binding cleft revealed a few exposed aromatic residues. Substitutions of certain amino acids in the surface and loop regions of CHI II conferred an increased flexibility to the enzyme, allowing for an adaptation to cold temperatures. A substrate binding comparison of CHI II with the mesophilic chitinase from *Coccidioides immitis*, 1D2K, suggested that the psychrophilic adaptation and catalytic activity at low temperatures were achieved through a reduction in the number of salt bridges, fewer hydrogen bonds and an increase in the exposure of the hydrophobic side chains to the solvent.

Keywords Chitinase · Psychrophilic · 3D model · Cold adaptation · Flexibility

A. N. M. Ramli · R. Md. Illias (✉)
Department of Bioprocess Engineering, Faculty of Chemical Engineering, Universiti Teknologi Malaysia, 81310 Skudai, Johor, Malaysia
e-mail: r-rosli@utm.my

N. M. Mahadi
Malaysia Genome Institute (MGI), Jalan Bangi Lama, 43000 Kajang, Selangor, Malaysia

M. S. Shamsir · K. H. Joyce-Tan
Faculty of Bioscience and Bioengineering, Universiti Teknologi Malaysia, 81310 Skudai, Johor, Malaysia

A. Rabu · A. M. A. Murad
School of Biosciences and Biotechnology, Faculty of Science and Technology, Universiti Kebangsaan Malaysia, 43600 Bangi, Selangor, Malaysia

Introduction

There has been a growing interest in psychrophilic enzymes in recent years because these enzymes can be used to improve the efficiency of industrial processes, in environmental applications, as potential candidates for biotechnology applications and for protein structure–function studies [1]. Structural comparisons of psychrophilic, mesophilic, thermophilic and hyperthermophilic enzymes have identified the mechanisms that underlie the thermoadaptation of the catalytic mechanism and their thermostability factors. X-ray structures of cold-active enzymes have revealed new insights into the mechanism of psychrophilic adaptation in proteins [2, 3]. Psychrophilic enzymes are often characterised by a high flexibility that enables both thermolability and a high catalytic efficiency at low temperatures. Increased structural flexibility in psychrophilic enzymes is achieved through a combination of structural features, such as a decrease in the proline and arginine content of the sequence, an increase in the glycine content of the sequence, a weakening of the intramolecular bonds through a reduction in the number of hydrogen bonds and salt bridges, an increase in the number of hydrophobic side chains that are exposed to the solvent,

longer and more frequent hydrophilic loops and a decrease in the compactness of the hydrophobic core [3, 4].

Chitinases hydrolyse the β-1,4-glycosidic linkages of chitin, which is a homopolymer of N-acetylglucosamine. The enzymes belong to families 18 and 19 of the glycoside hydrolases. Chitinase family 18 has been identified in a variety of organisms, including fungi, insects, plants, viruses and animals [5]. The catalytic domain of the family 18 chitinases have a $(\beta/\alpha)_8$ fold (TIM barrel) and contain a characteristic DXDXE sequence motif, which is involved in catalysis [6]. Studies of fungal chitinases have suggested that psychrophilic chitinases are responsible for many important biological and physiological functions under these low-temperature conditions, including autolysis, nutrition, morphogenesis and parasitism. Many psychrophilic chitinase enzymes have been reported in bacteria [5, 7], plants [8] and fungi [9].

Knowledge and information about the detailed structural organisation of proteins is crucial in understanding their role in the cell and in other related molecular mechanisms [10]. This task can be facilitated by determining the accurate three-dimensional (3D) structure of the studied protein. Recently, the prediction of protein structure has attracted a considerable amount of attention, as documented by the emergence of new prediction methods [11–15]. Comparative modelling or homology modelling can help develop a useful 3D model for a protein's structure in the absence of an experimentally determined structure [16]. The application of comparative modelling in cases with high sequence identities (more than 35 %) typically results in accurate models. However, in cases of low sequence identity (<30 %), threading might offer a more accurate solution. In threading, structural information is used to compare an amino acid sequence to a library of known folds [17].

Until recently, the 3D structure of cold-adapted chitinases from psychrophilic yeast remained to be identified. In this paper, we modelled the structure of a novel chitinase, CHI II, from *G. antarctica* PI12. The predicted 3D model of this novel enzyme was analysed structurally and simulated using molecular dynamic simulation. In an attempt to clarify the potential psychrophilic adaptations of the CHI II chitinase enzyme, the primary sequence and predicted structure of the protein were compared to other mesophilic and thermophilic chitinases. Several characteristics were identified that may have a great impact on the thermolability of this enzyme.

Materials and methods

CHI II data mining

The psychrophilic yeast strain, *G. antarctica* PI12, was obtained from the School of Biosciences and Biotechnology, Universiti Kebangsaan Malaysia, Malaysia. The full-length gene for the novel chitinase from *G. antarctica* PI12, CHI II, was isolated using rapid amplification cDNA Ends (RACE) [18]. The complete sequence has been deposited in the GenBank database under accession no. JF901326. The resulting amino acid sequence (404 residues) was subjected to various sequence analyses with BLAST-PDB [19] and PSI-BLAST [20], while SUPERFAMILY HMM [21] was used to identify any possible families or conserved domains in the protein.

Model development and evaluation

Threading was performed by submitting the amino acid sequence (excluding the signal peptide) to the library of known folds using Phyre [11], HHpred [12], PSI-BLAST, mGenThreader [13] and Modlink+ [14]. The sequence-structure alignment was optimised using the threading method, and this alignment was used as the input for the development of 3D models using MODELLER9v7 [15]. We generated 100 models and used MODELLER9v7 for each alignment. The model with the lowest objective function was selected and evaluated based on its root-mean-square deviation (RMSD) and Tm-score [22]. The Tm-score result was obtained from the Tm-align program [23]. TM-align is a structural alignment program that compares two proteins with different sequences. TM-align will first find the best equivalent residues of the two proteins based on the structural similarity and then output a TM-score. Optimisation and energy minimisation of the resulting models was performed using CHARM-22 from Accelrys Discovery Studio 2.5 and the steepest descent algorithm implemented in GROMOS from Deepview [24]. The protein structure assessment tools used were PROCHECK [25], VERIFY-3D [26], ERRAT [27] and ProSA-web [28].

Molecular dynamic (MD) simulations of CHI II

In the MD simulations, the modelled CHI II structure was simulated using the GROMACS MD simulation software to examine the structural stability at three different temperatures: a low temperature of 273 K (0 °C), the working temperature (optimum temperature) of 288 K (15 °C) [18] and a moderate temperature of 300 K (27 °C). Simulation at these three different temperatures is expected to show a discernible MD stability profile. CHI II was solvated in a box of explicit simple point charge (SPC) water molecules and simulated using periodic boundary conditions (PBC) and particle mesh Ewald (PME) summation to improve electrostatic interactions [29]. Structures were minimised using 200 steps from the steepest descent method. Simulations were performed using the GROMACS 4.5.3 package and the all-hydrogen function, GROMOS96 [30].

Simulations were conducted at 273, 288 and 300 K, and isotropic pressure coupling was applied. All systems were equilibrated for 200 ps of solute position-restrained MD. Unrestrained MD was performed on all variants for 10 ns with a LINCS algorithm 2-fs time step for each system. All of the resulting trajectories were analysed using GROMACS utilities. The Javis Patrick clustering method available through the g_cluster tool in GROMACS was employed to group the conformations using RMSD cut-off values of 0.1 nm to arrange the neighbouring structures. During the cluster formation, the number of nearest neighbours in a list was set at 10, while the number of nearest neighbours in common for conformations in a list to be clustered was set at 3 (data not shown). The central structure from the most populated cluster at these simulations was then used as the reference structure in the backbone and C_β root mean square deviations (RMSD) analysis. Cα root mean square fluctuations (RMSF) relative to the initial structure were calculated.

Structural comparison of CHI II with regard to cold adaptation

The solved crystal structure of chitinase from *Coccidioides immitis* (1D2K), obtained from the PDB database, was used as a reference for structural comparison. Salt bridges were analysed by the ESBRI program [31]. A salt bridge was defined as an ion pair with a distance of 2.5–4 Å between the charged, non-hydrogen atoms. A distance cut-off was applied to the carboxylate oxygen atoms of Glu and Asp and the NE, NH1 and NH2 groups of Arg [32]. The hydrogen bonds and the accessible surface area were calculated using Accelrys DS studio 2.5. For hydrogen bonds, a cut-off distance of 3.3 Å between the hydrogen donor and the hydrogen acceptor atoms was used. All of the graphic presentations of the 3D model were prepared using Deepview and PyMOL [33].

Results and discussions

CHI II data mining

Our analysis of the CHI II sequence showed that the psychrophilic CHI II protein lacked similarity with all known structures in the PDB. The BLAST and PSI-BLAST results revealed that CHI II exhibits low similarity with all solved 3D structures in the PDB database, with the highest match showing only 30 % identity and 45 % similarity to chain A of the catalytic domain of chitinase A1 from *Bacillus circulans*. Using the SUPERFAMILY HMM library and the genome assignments server, we found that the CHI II enzyme belongs to the TIM barrel family, as demonstrated by the conserved domain search.

Template selection

Because of the low percentage of identity in the sequence alignment, which was less than 30 % (the 'twilight zone'), the first two steps in the homology modelling were substituted for the fold recognition, or threading, method. A previous study by Schoonman et al. [17] confirmed that threading methods are able to yield more accurate models than comparative modelling in cases of low sequence identity (<30 %). An evaluation was performed using several threading programs, including Phyre, HHpred, PSI-BLAST, mGenThreader and Modlink+. The results from the threading programs were compared and analysed as shown in Table 1.

Of the templates compared (Table 1), only the catalytic domain of chitinase A1 from *B. circulans* WL-12 (1ITX) appeared in the all of the results given by the different methods; it was either the best or the third best match in all cases. This template was determined to be in the same TIM barrel family as CHI II. As 1ITX gave the best sequence and structural alignments, it is a suitable template for CHI II. Other templates did show a higher sequence identity to CHI II compared to 1ITX. For example, 1JND and 1W9P showed a 23 and 22 % identity to CHI II, respectively. However, the reliability of the alignment was in doubt, as the sequence-structure alignments produced between CHI II and these templates contained numerous insertions and deletions that could cause catastrophic problems in the construction of a 3D model. Therefore, 1ITX was chosen as the model template for CHI II.

To further assess the reliability of the structural sequence alignment between CHI II and 1ITX, the consensus secondary structure prediction was used to confirm the alignment (Fig. 1). This was achieved by comparing the aligned secondary structure of 1ITX and the consensus predicted secondary structure of CHI II. The structural alignment showed a good alignment at 8 α-helices and 9 β-strands between CHI II and 1ITX. The rest of the proteins' regions were shown to consist of random coils and a few structural mismatches and gap-containing segments. The long gap of CHI II that starts at residue number 61 will be discussed in the CHI II model analysis section.

3D model building and refinement

To select the best sequence-structure alignments between CHI II and 1ITX, the alignment results from different threading programs were used to build models with MODELLER. MODELLER is a program that works based

Table 1 Proposed template structures obtained from different threading methods along with their calculated scores. ITX appeared in the all of the results given by the different methods and was chosen as the model template for CHI II

Program	Template	Protein characteristics	Fold	% identity	Score (*E* value[a])
Phyre	1ITX	Chitinase A1	Tim Barrel	23	7.3e−29
	1NWU	Human cartilage gp39	Tim Barrel	23	8.7e−29
	3CHC	Chitinase B1	Tim Barrel	21	1.2e−28
HHpred	1ITX	Chitinase A1	Tim Barrel	28	0
	3B9E	Chitinase A	Tim Barrel	23	0
	1EDQ	Chitinase A	Tim Barrel	23	0
PSIblast	1ITX	Chitinase A1	Tim Barrel	30	4e−29
	1LQO	Fosfomycin resistance protein	Glyoxalase	28	7e−27
	1GUV	Chitotriosidase	Tim Barrel	28	9e−27
mGenThreader	1JND	Imaginal disc growth factor-2	Tim Barrel	23	7e−09
	2PI6	Chitinase-3-like protein 1	Tim Barrel	22	1e−08
	1ITX	Chitinase A1	Tim Barrel	20	3e−06
ModLink+	1W9P	Chitinase	Tim Barrel	22	3e−74
	1VF8	Chitinase-like lectin	Tim Barrel	22	1e−72
	1ITX	Chitinase A1	Tim Barrel	20	2e−72

[a] *E* value must be as low as possible

on the satisfaction of spatial restraints; the program satisfies all the restrains derived from the structure-sequence alignment. Models that produced high violations of the restraints are considered poor, and those models led to higher objective functions, such as by the CHARM-22 force field [34]. Manual adjustment of the gap was performed to improve the alignment. The models with the lowest objective function from the different alignments were then evaluated based on their RMSD and TM-score by comparing the model to the template. The TM-score is an algorithm to calculate the similarity between two protein structures and is widely used to measure model quality. The TM-score is more sensitive than the RMSD because the TM-score weights closer matches more strongly than distant matches [35]. The TM-score falls between 0 and 1, where a score of 0 to roughly 0.2 is considered a random hit and a score above 0.4 is considered meaningful. The predicted quality was used to rank all of the alignments for a given target, as shown in Table 2.

Table 2 shows that alignment performed by the Phyre program produced the best model, with a RMSD of 1.45 Å, a Tm-score of 0.83077 and the highest coverage of the aligned length compared to the other proposed models. Although it has the lowest RMSD, the model generated from the alignment performed by PSIblast and ModLink+ was found to have the lowest aligned length and was therefore not very significant.

The Phyre alignment model was subjected to energy minimisation using the steepest descent algorithm as implemented in GROMOS from Deepview to avoid poor molecular contacts. Side-chain and loop refinement of the resulting model was then performed by CHARM-22 from Accelrys Discovery Studio 2.5.

Quality of the model

The quality of the model with regard to the refined structure was evaluated using PROCHECK, VERIFY3D, ERRAT and ProSA-web. The backbone conformation was evaluated by inspecting the Psi/Phi Ramachandran plot obtained from the PROCHECK analysis. The PROCHECK analysis shown only three residues that were located in the disallowed region (Ser9, Leu53 and Cys224); 85.6 % of the residues were located in the most favoured region, and the remaining residues were found to reside in the additional and generously allowed regions. VERIFY3D analysis shown that 85.75 % of the residues had an average 3D–1D score greater than 0.2, indicating that only 14.25 % of the residues did not complement the 3D–1D profile. A VERIFY3D score of greater than 80 % indicates that the predicted model is of satisfactory quality [26]. The ERRAT score was found to be 72.603. ERRAT is the overall quality factor for nonbonded atomic interactions and is calculated by a comparison of statistics with highly refined structures. Higher ERRAT scores indicate a higher quality, and the normally accepted range for a high quality model is >50 % [36]. In addition, model assessment was also performed using ProSA-web to calculate an overall quality score for a specific input structure. If this score is outside a range characteristic for native proteins, the structure most likely contains errors. The *z*-score of the input model (CHI II)

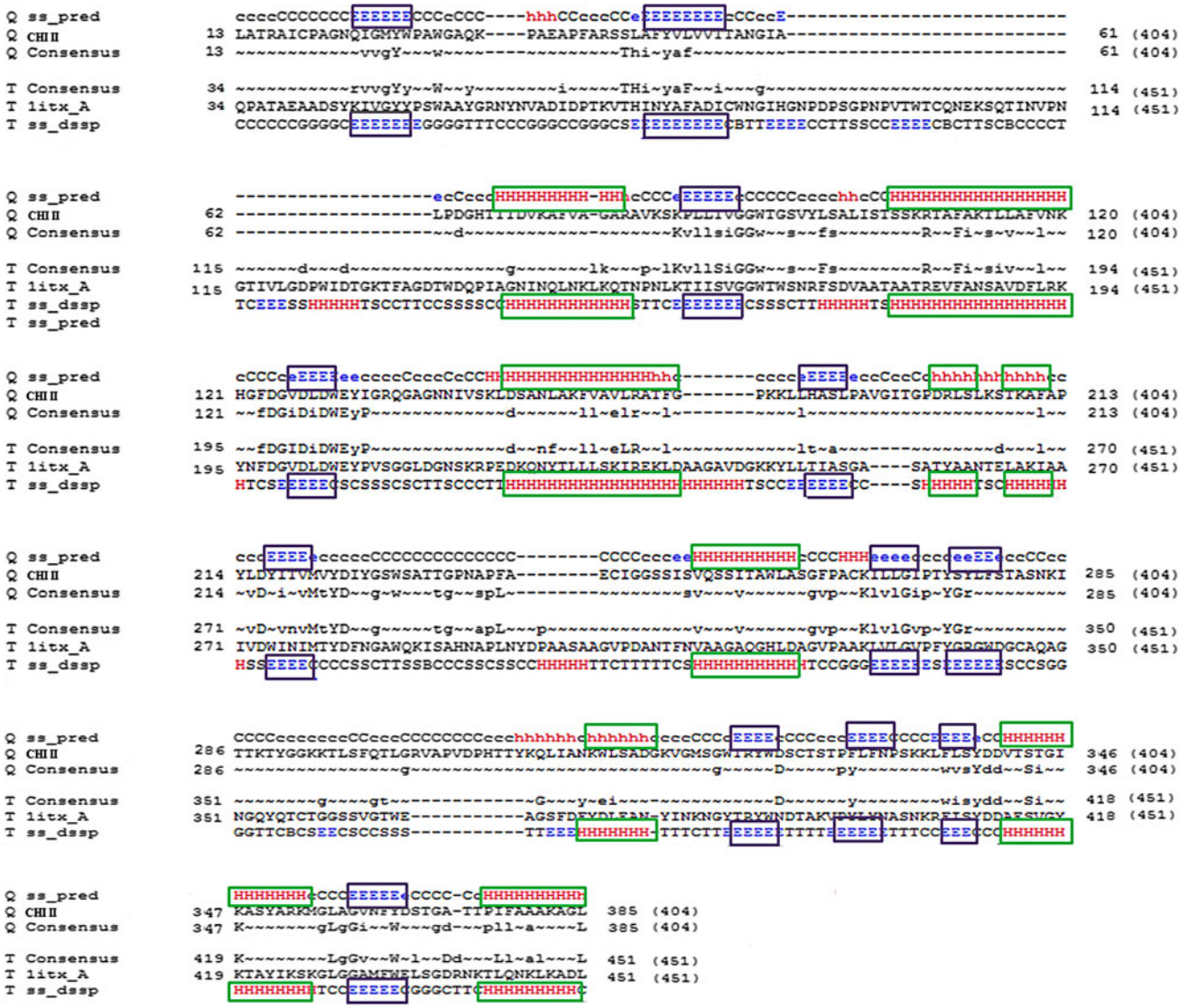

Fig. 1 Sequence-structure alignment between CHI II and 1ITX. The *purple* and *green* boxes represent the aligned secondary structure elements between the two proteins (helices and β-strands, respectively). Regions containing loops or random coils also aligned very well between the two proteins. (Q CHI II—Consensus secondary structure prediction for CHI II; T 1itx_A—Secondary structure of 1ITX)

was found to be −7.17, which is within the range of scores typically found for native proteins of a similar size.

Overall, the values obtained from the evaluation programs appeared reasonable, after taking into account that the structure of CHI II was obtained using the threading method with a low sequence identity (<30 %) and a low sequence similarity (45 %) between the template and target proteins.

CHI II model analysis

Figure 2 shows a representation of the CHI II 3D model. The model has features similar to those of other members of the class 18 hydrolase family for which crystal structures have been identified [37, 38]. Proteins that belong to the class 18 family of chitinases have two signature sequences (XXGG and DXXDXDXE) [39], corresponding to residues 90–96 and 125–132 in CHI II, where the residue numbering was based on the mature amino acid sequence of CHI II. As in the other chitinase structures found in the literature, these residues lie along the barrel strands 3 and 4 (S3 and S4) and help to form the active site cleft on the carboxyl end of the β-barrel [37, 40]. The catalytic domain of CHI II has a conserved $(\beta/\alpha)_8$ fold that is considered a TIM barrel, as it includes an alternating pattern of α-helices and β-strands within a single domain. The TIM-barrel structure is known as a general folding motif of family 18 chitinase because it has been found in most of the solved chitinase

Table 2 Evaluation analysis of the models from the alignment results from the different threading programs

Program	Best model[a]	Evaluation
Phyre	35.pdb	RMSD = 1.45
		Tm score = 0.83077
		Aligned length = 356
HHpred	84.pdb	RMSD = 1.53
		Tm score = 0.82368
		Aligned length = 351
PSIblast	74.pdb	RMSD = 0.84
		Tm score = 0.91722
		Aligned length = 264
mGenThreader	89.pdb	RMSD = 1.94
		Tm score = 0.79986
		Aligned length = 349
ModLink+	20.pdb	RMSD = 1.22
		Tm score = 0.56069
		Aligned length = 239

[a] Best Model = Model with the lowest DOPE score and highest GA341 score among 100 model generated by MODELLER

structures [39, 40]. The parallel β-strands that form the core of the enzyme are labelled S1–S9, and each of these strands is followed by a-return α-helices labelled H1–H10.

The superimposition of the 3D CHI II model with the structure of 1ITX (Fig. 3a) yielded an RMSD of 1.45 Å that covered 63.37 % of the backbone atoms, indicating a good overall structure alignment. The proposed catalytic residues for the modelled CHI II structures (Asp125–Glu132) are represented as sticks and fall into approximately the same locations as in 1ITX (Fig. 3b). The conservation of the catalytic residues and the identical structural assignments in the modelling suggest that the modelled chitinase structure is an accurate representation of the actual protein's structure.

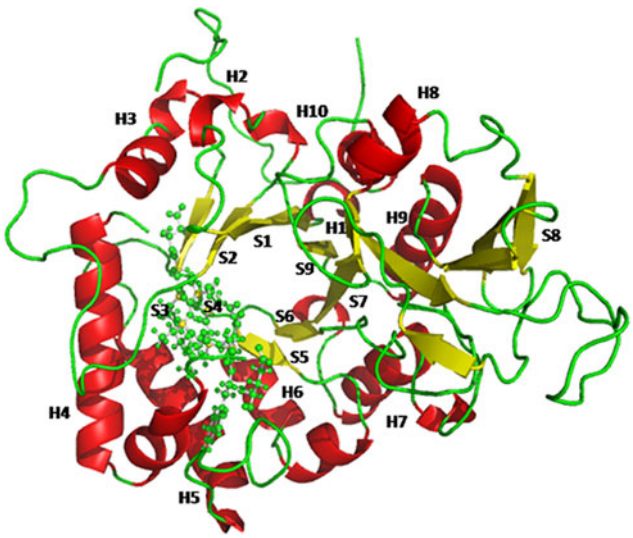

Fig. 2 3D model of CHI II with the β strands, S1–S9 and the α helices, H1–H10, labelled. Two signature sequences (XXGG and DXXDXDXE) corresponding to residues 90–96 and 125–132 of CHI II are represented as *balls* and *sticks*

The 1ITX template consists of an α/β-barrel and two small β-domains (β-domain 1 and β-domain 2) attached at the top of the α/β–barrel domain, which provides a deep cleft for substrate binding [38]. The α/β-barrel domain of 1ITX is similar to the so-called TIM-barrel structure. The long gap of CHI II that starts at residue number 61 is located in the region between residue numbers 87–133 of 1ITX. Interestingly, this region in 1ITX corresponds to the region for one of the small β-domains, β-domain 1. Therefore, the two catalytic domains of CHI II and 1ITX have essentially the same structure, as expected from their similarity in their secondary structure alignment (Fig. 1), except that CHI II lacks β-domain 1, as shown in Fig. 4.

The two small β-domains are commonly present in microbial chitinase enzymes such as those from *B. circulans* [41] and *Serratia marcescens* [42]. The two β-domains are located separately on top of the Tim-barrel and provide a cleft for substrate binding. CHI II chitinase lacks β-domain 1 and was found to have only β-domain 2 in the predicted structure. β-domain 1, which is usually found in bacterial chitinases, has a fold comprised of only β-strands. This domain is not involved in saccharide binding [43]. No biochemical data have been available regarding the function of this domain [42]. β-domain 2, which is also found in mammalian lectin [43] and a chitinase from *C. immitis* [37], includes the chitinase insertion domain (CID) region. CID is also known as an ($\alpha + \beta$) insertion in the TIM-barrel catalytic domain. The CID in CHI II is formed by an insertion between β-strand 7 (S7) and α-helix 7 (H7) comprised of residues 255–357. It contains six β-strands and one helix and forms a deep substrate-binding cleft that is assumed to be important in processive hydrolysis of the chitin chain [41]. The TIM-barrel domain plus the CID domain can bind long chain substrates by providing a deep substrate binding cleft, which may not be the case for enzymes containing only the TIM-barrel domain [44], e.g., plant chitinase (hevamine) [39]. In general, additional modules fused to a catalytic domain may play a role in substrate specificity by providing a specific binding site or shaping the active site to recognise a substrate with a different shape or size [41]. Several differences can be noted between the CID from CHI II and those found in other chitinases. A previous study revealed that the CID has a large percentage of aromatic residues, for example, 21 % in *B. circulans* and 23 % in *Thermococcus kodakarensis* [44]. Only 17 % of the CID from CHI II is composed of aromatic residues. These aromatic residues have been found to play an important role in stabilising proteins and

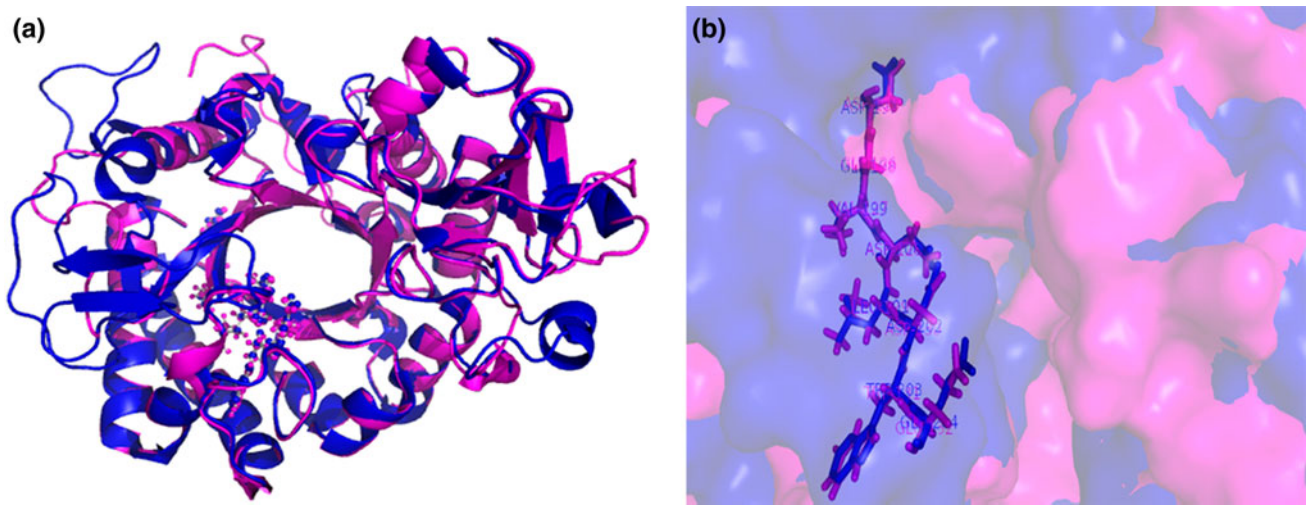

Fig. 3 **a** Superimposition of the refined CHI II model and its template, 1ITX. Both structures are shown in a cartoon representation. The *blue ribbon* represents the 1ITX structure, while the *magenta ribbon* represents the CHI II model. The catalytic regions of both models are represented as *balls* and *sticks*. **b** Close-up view of the CHI II catalytic residues (Asp125–Glu132) compared to the 1ITX catalytic residues (Asp197–Glu204)

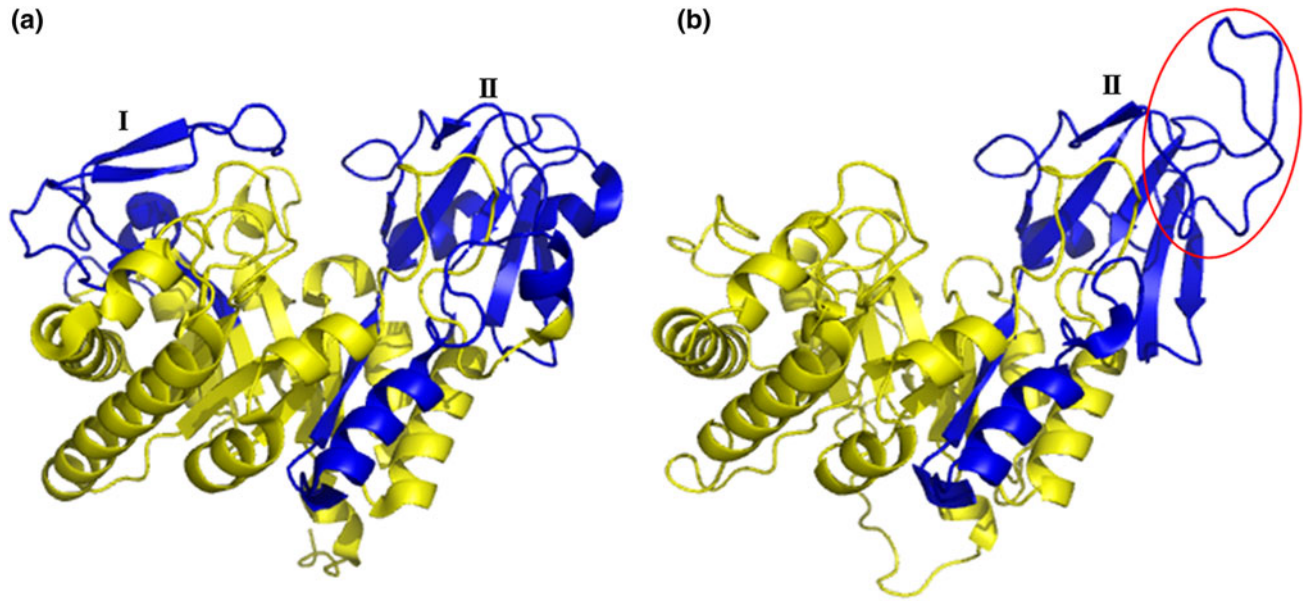

Fig. 4 **a** The 3D structure of 1ITX consists of an α/β-barrel (*yellow*), β-domain 1, labelled as I (*blue*) and β-domain 2, labelled as II (*blue*), which provides a deep cleft for substrate binding. **b** The 3D model of CHI II consists of an a/β-barrel (*yellow*) and β-domain 2, labelled as II (*blue*), in the absence of β-domain 1. The longer hydrophilic loop at residues 261–284 in CHI II is circled in *red*

peptides [45]. Therefore, the reduced aromatic residue content in the CID of CHI II will decrease its thermal stability, making this CID more flexible for substrate binding in cold temperatures. In addition to that difference from other mesophilic and thermophilic organisms [44], the CID from CHI II was found to contain a longer hydrophilic loop at residue 261–284 (Fig. 4). It was proposed that the higher structural flexibility of psychrophilic enzymes compared to their mesophilic and thermophilic counterparts might be the result of a combination of several features, including longer and more hydrophilic loops [3]. Therefore, this loop might be responsible for the flexibility of the CHI II structure, which contributes to its adaptation to low temperatures.

Structural analysis of the CHI II substrate-binding cleft

Analysis of the CHI II 3D model revealed a few exposed aromatic residues, including Trp92, Trp204, Trp210 and Tyr362, which are all conserved and linearly align with the

aromatic residues at the binding clefts of *B. circulans* chitinase A1 [41] and *S. marcescens* chitinase A [46]. Previous studies using site-directed mutagenesis of *B. circulans* and *S. marcescens* 2170 [47] chitinases suggested that these surface-exposed aromatic residues are important for guiding the chitin chain to the catalytic cleft so that effective catalysis can take place. As stated in the 3D model building and refinement section, the catalytic domain of chitinase A1 from *B. circulans* WL-12 (1ITX) was chosen as the template for building the 3D model of CHI II. Inactivation studies of the catalytic domain of chitinase A1 from the *B. circulans* WL-12 complex with $(GlcNAc)_7$ have been carried out by Watanabe et al. [48]. Based on this study, four aromatic residues that are involved in the interaction with the sugar ring at subsites −2, −1, +1 and +2 were identified. Comparison of the CHI II chitinase with the catalytic domain of chitinase A1 from *B. circulans* WL-12 revealed that Trp92, Tyr204, Trp210 and Tyr362 in CHI II might have the same functions as Trp164, Trp285, Tyr279 and Trp433 in *B. circulans* WL-12 chitinase A1, as shown in Fig. 5. Trp164 and Trp285 (equivalent to Trp92 and Tyr204 in CHI II) in *B. circulans* WL-12 chitinase A1 are very important for crystalline chitin hydrolysis and also participate in the hydrolysis of other substrates. Similarly, Tyr279 and Trp433 (equivalent to Trp210 and Tyr362 in CHI II) are conserved in all family 18 chitinases [41], which is in agreement with an essential role for these two residues in the catalytic reaction [47]. In addition, we found another surface-exposed aromatic residue in CHI II at the edge of substrate-binding cleft, Trp32, that is linearly aligned with the other aromatic residues in the binding cleft and may contribute to substrate binding or function in crystalline-chitin hydrolysis (Fig. 5).

Molecular dynamic simulations: structural deviations, fluctuation and evaluations

In this paper, we performed MD simulation of CHI II at three different temperatures, 273, 288 and 300 K. Throughout the 10 ns simulation, 5,000 conformations were produced during each simulation. To analyse the stability of the modelled CHI II structure, a non-hierarchical clustering method, the Jarvis-Patrick algorithm [49], which is available through the g_cluster tool in GROMACS, was employed to cluster similar conformations in the produced trajectories. During cluster analysis, RMSD would normally be the measurement while torsion angles serve as another alternative. A more stable structure at a particular temperature is expected to form fewer clusters. The Jarvis-Patrick method uses the 'nearest neighbours' approach, where similarity matrix is first built, followed by cluster formation based on evaluation of the nearest neighbours of each conformation. The cluster is then fused together when a sufficient number of common nearest neighbours matched the criteria. Cluster analysis performed on conformations ensembles produced at these three temperatures grouped the matching conformers into one (273 K), five (288 K) and eight clusters (300 K), respectively. The central structure of the most populated cluster of these simulations was then used as the reference structure in RMSD analysis (Fig. 6a). The RMSD value of the CHI II predicted structure was found to be the lowest at 273 K, followed by 288 and 300 K. The average RMSD for the structure at 273, 288 and 300 K were 2.85, 4.15 and 5.31 nm, respectively. At 273 K, the RMSD of the CHI II model experienced a sharp decrease at 1.8 ns and stabilised for 4 ns before increasing gradually and stabilising at 8.2 ns. The RMSD value at 288 K was constant before decreasing after 7.2 ns. In the 300 K simulation, the RMSD fluctuated throughout the simulation. At the end of the simulation, convergence of the RMSD value of CHI II can be observed in the simulation performed at 273 and 288 K. From the cluster and RMSD analysis, the structure at 288 K was more stable compared to the structure at 273 and 300 K. This structure had the most consistent RMSD plot, and the RMSD standard deviation at the function of time was the lowest for 288 K (0.44) compared to 273 K (0.58) and 300 K (0.59). Although the structure at 273 K displayed a lower RMSD value compared to the structure at 288 K, its enzymatic activity was limited to 23 % when determined experimentally at 5 °C [18]. Thus, similar enzymatic activity or even lower observation would be expected for CHI II at 273 K. In addition, the RMSF of the C_α atom of CHI II from the initial structure as a function of residue number at 273, 288 and 300 K was plotted to evaluate the average fluctuation of each residue during the simulation (Fig. 6b). The RMSF of the Cα value of the CHI II structure at 273 K was comparable to the structure at 288 K, except a higher value was observed at residue 7–19 and 57–81, both of which are coil regions. At 300 K, the Cα of CHI II generally exhibited a higher fluctuation. A similar fluctuation pattern could be observed in these three simulations, with the highest fluctuations occurring at the N terminus and in the loop between secondary structure elements. The CHI II secondary structure fluctuations behaved similarly at all temperatures tested; higher fluctuations occurred in the loops, creating identical peak and groove signatures. Enhanced localised flexibility in the loop regions of CHI II confers a greater flexibility to the CHI II enzymes. A similar finding has been reported in a comparative molecular dynamics study of the psychrophilic and mesophilic antifreeze proteins from *Macrozoarces americanus* and humans, respectively, where the localised flexibility in the loop region of the psychrophilic antifreeze protein at 277 and 298 K was greater than the flexibility in

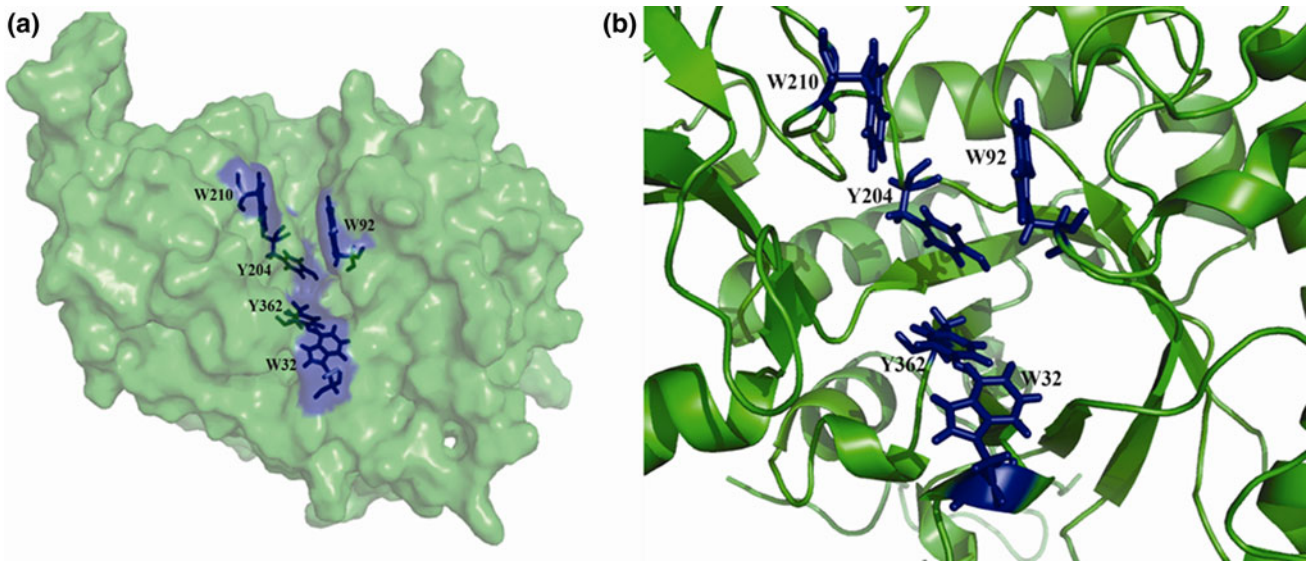

Fig. 5 **a** A surface representation showing the positions of the aromatic residues at the substrate-binding cleft of CHI II. **b** Close-up view of the CHI II substrate-binding cleft, with the linearly aligned aromatic residues involved in substrate-binding activity shown as a side chain. *W* corresponds to Trp, while *Y* corresponds to Tyr

the mesophilic protein [50]. Therefore, this suggests that improved flexibility of the loop regions in CHI II could be a contributor to its adaptation to cold. The evolution of the secondary structures during the MD simulation was determined by the database of secondary structure assignments (DSSP). Both simulations show that the global conformation of CHI II is stable, with no significant changes in its secondary structure elements.

Comparison based on primary sequence analysis of CHI II for cold adaptation

Examination of the psychotropic characteristics of CHI II using an amino acid sequence alignment of psychrophilic, mesophilic and thermophilic chitinases showed that the catalytic residues are conserved between all of the examined chitinases (Fig. 7). Previous research has shown that each cold-adapted enzyme uses different small selections of residue changes that result in structural adjustments. These adjustments typically increase the molecular flexibility, which in turn gives rise to increased catalytic efficiency and reduced stability at certain protein regions [32]. The multiple sequence alignment of CHI II with other psychrophilic, mesophilic and thermophilic chitinases in Fig. 7 reveals several interesting substitutions of the signature psychrophilic amino acid residues.

Proline is an imino acid, as its side chain is covalently linked to its backbone. The pyrolidine ring of proline severely restricts the possible conformations of the preceding residue. The presence of proline increases both protein stability and local rigidity by reducing the configurational entropy of unfolding and constraining the flexibility of the main chain [51]. Proline substitution is closely related to flexibility, and proline substitutions were found at positions 76, 120, 153, 197, 247 and 317 of CHI II, where prolines that are conserved throughout the mesophilic and thermophilic chitinases were replaced by other hydrophobic amino acid residues (alanine, isoleucine and leucine), as shown in Table 3. The substitutions of hydrophobic residues were found to be important for generating the flexibility of CHI II. These hydrophobic surface residues destabilise the protein's structure due to the decreased entropy of the water molecules [52]. Substitutions in the loop regions were observed at positions 85, 153 and 196, which are located on the surface of the molecule and in the vicinity of the substrate-binding cleft. The substitution of proline residues in the loop regions had a stabilising effect, which may allow a higher flexibility of the substrate binding cleft, enabling the enzyme to catalyse reactions at lower temperatures [53]. The side chain of the proline residues is covalently bound to the N atom of the peptide backbone, thereby restricting the rotation about N–C_α bonds and reducing the conformational flexibility of loop structures [54]. Therefore, the plasticity or flexibility of CHI II can be attributed to an increased flexibility at an appropriate portion of the molecular structure, which compensates for the lower thermal energy provided by the low-temperature habitat. However, there are some locations in the psychrophilic CHI II (49, 82, 104, 193, 309 and 389) that exhibited proline residues that are replaced by other residues in equivalent positions of mesophilic and thermophilic chitinases. This observation will support the

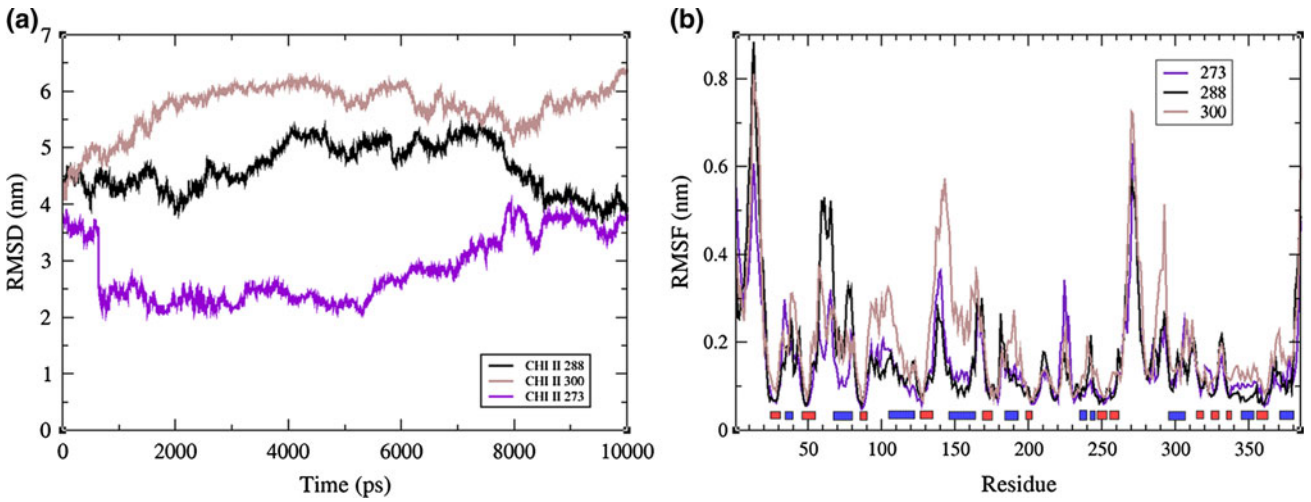

Fig. 6 **a** RMSD using a central structure from the most populated cluster by cluster analysis as the reference structure CHI II as a function of time at 273 K (0 °C), 288 K (15 °C) and 300 K (27 °C). CHI II simulated at 288 K, its optimum temperature, displayed a more consistent RMSD value compared to the structures simulated at 273 and 300 K. **b** RMSF of the C_α atom of CHI II from the initial structure as a function of residue number at 273, 288 and 300 K. The structure simulated at 300 K generally exhibited higher fluctuations, while the structure simulated at 273 and 288 K displayed a similar fluctuation pattern

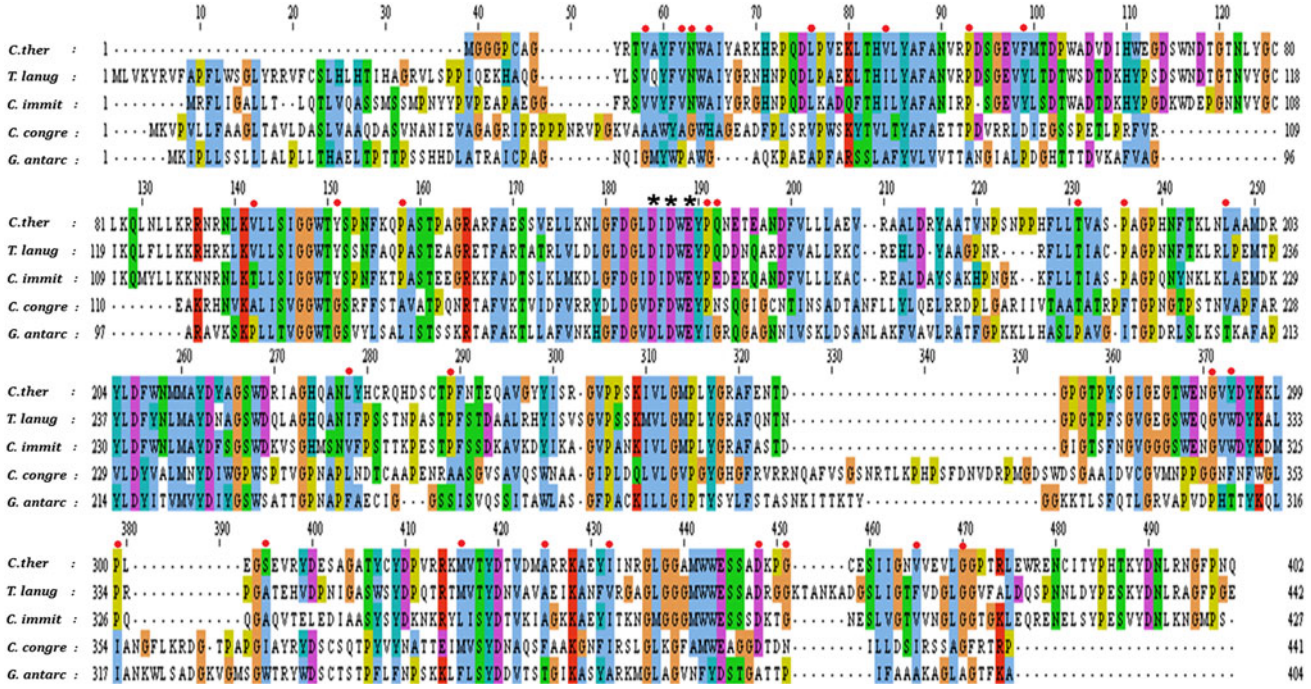

Fig. 7 Alignments of amino acid sequences of chitinases from mesophiles: *C. immit* (*Coccidioides immitis*; AAA92643) and *C. congre* (*Coprinellus congregates*; CAQ51152); thermophiles: *C. ther* (*Thermoascus aurantiacus var. levisporus*; ABS00927) and *T. lanug* (*Thermomyces lanuginosus*; AAY99632), and a psychrophile: *G. antarc* (*G. antarctica* PI12; AEH16745). The conserved catalytic residues, Asp128, Asp130 and Glu132, are indicated with stars. *Red dots* (*filled circle*) indicate the locations of amino acid substitutions

hypothesis that psychrophilic enzymes are characterised by an improved flexibility of the structural components involved in the catalytic cycle, whereas other protein regions, if not implicated in catalysis, may be as or more rigid than their mesophilic counterparts [55]. In addition, for the optimal enzyme catalysis at low temperatures, a proper balance between structural rigidity and flexibility is important to allow the retention of a specific 3D conformation at the physiological temperature and to enable the protein to perform its catalytic function. Previously, several studies have focused on whether cold-adapted proteins have flexibility throughout their structure (global flexibility) or

whether they have distinct regions of local flexibility [56]. Although global flexibility has been shown to promote high activity and low stability in cold-adapted enzymes, it may also increase the possibility of incorrect folding [53]. Thus, to attain sufficient activity at low temperatures, the active site cleft of cold-adapted enzymes may need to be more flexible than peripheral parts of the enzyme.

In addition to proline, there are other substitutions of CHI II amino acids that confer protein stability to appropriate regions. These substitutions involved aromatic residues (phenylalanine and tryptophan) in CHI II. These residues occurred at positions 239, 333, 354 and 391, and mesophilic and thermophilic chitinases have other residues at structurally equivalent positions, such as valine, alanine, leucine, methionine, serine and isoleucine. The aromatic rings (usually found in tryptophan, tyrosine and phenylalanine) have a dipole because of the partial negative charge on the face of the ring caused by the π-electron cloud and by a partial positive charge on the C–H edges. This polarity permits two favourable interactions: aromatic–aromatic interactions and aromatic-amino interactions, which occur between aromatic rings at right angles to each other or between aromatic rings and the side chains of arginine and lysine, respectively. Aromatic interactions may therefore promote thermostabilisation through an enthalpic contribution [53]. Comparison analysis of two homologous families of psychrophilic and mesophilic water-borne signal proteins showed that psychrophilic proteins contain more aromatic residues compared with their mesophilic homologs. This suggests that, at low temperature, some cold-adapted proteins need to maintain their protein folds while at the same time allow an increase in local structural flexibility to enable effective protein activity [57]. The diverse activation strategies used by psychrophilic enzymes in colder environments have resulted in a number of divergent viewpoints on the influence of local and global protein flexibility on cold adaptation.

Glycine is thought to modulate the entropy of protein unfolding by affecting the flexibility of the backbone [58]. The main chain of glycine has more conformational freedom because the lack of a side chain allows chain rotations and dihedral angles that are not available to other amino acids [2]. Substitutions of amino acids to glycine occurred at positions 45, 52, 113 and 153 of CHI II, where mesophilic and thermophilic chitinases have other residues at structurally equivalent positions, such as valine, alanine, histidine and tyrosine (Table 3). It has been suggested that the stacking of glycine around the catalytic residues (positions 114 and 159) improves the flexibility of the active site [58]. Therefore, the replacement of tyrosine and alanine with Gly114 and Gly159 in CHI II, respectively, may contribute to the high catalytic efficiency of CHI II at low temperatures.

Table 3 Amino acid substitutions in CHI II compared to the equivalent locations in mesophilic and thermophilic chitinases. The comparison and analysis were performed based on the amino acids sequence alignment in Fig. 7

Amino acid involved in thermostability/flexibility	Residue in mesophilic and thermophilic chitinase	Residue in psychrophilic CHI II
Proline residue	*Destabilizing effect*	
	Pro	Ala76
	Pro, Ala	Leu120
	Pro	Ile153
	Pro, Phe	Ile197
	Pro, Ala	Ser247
	Pro, Ile	Ile317
	Stabilizing effect	
	Ala, Val	Pro49
	Phe, Tyr, Asp	Pro82
	Val, Thr, Ala	Pro104
	Thr	Pro193
	Gly	Pro309
	Gly, Asn	Pro389
Aromatic residue	*Stabilizing effect*	
	Leu, Val, Ile	Phe239
	Ile, Ala, Ser	Trp333
	Leu, Met	Phe354
	Ile, Val, Leu	Phe391
Glycine residue	*Destabilizing effect*	
	Val, Ala	Gly45
	Ala, His	Gly52
	Tyr, Gly	Gly113
	Gln, Asn, Glu	Gly154
Hydrophobic residue	*Destabilizing effect*	
	Gly, Asn	Ala50
	Gln, Ser	Ala59
	Val, Ile, Leu	Ala67
	Ile, Val	Ala370
	Asp	Ala386
	Val, Phe, Ile	Ala394
	Gly	Ala399
Threonine residue	*Destabilizing effect*	
	Leu, Val	Thr208
	Tyr, Trp, Phe	Thr311
	Ala, Phe	Thr363

In addition, some other interesting substitutions were also determined from the multiple sequence alignment, including the replacement of large residues by tiny residues in the same hydrophobic group. Substitutions of amino acids to alanine occurred at positions 67, 370 and 394 of CHI II, whereas mesophilic and thermophilic chitinases had other hydrophobic residues at structurally equivalent

Table 4 Structural factors that are potentially involved in the weak thermal stability of the psychrophilic chitinase, CHI II

Parameters	CHI II	1D2K	Expected effect on CHI II stability
Salt bridges (formed by arginine residues)	5	6	Ionic interactions decrease
Hydrogen bond	126	187	Stability decrease
Accessible surface (Å^2):			
Total solvent accessibility	18,240	15,995	Stability decrease
Hydrophobic accessibility	3,779 (21 %)	1,122 (7 %)	
Hydrophilic accessibility	5,288 (29 %)	7,769 (49 %)	
Surface of positively charged aa (basic)	3,629 (20 %)	3,299 (21 %)	
Surface of negatively charged aa (acidic)	90 (5 %)	2,456 (15 %)	

positions, such as leucine, isoleucine, valine and phenylalanine (Table 3). A study from Zuber [59] found that comparison of the primary structures of lactate dehydrogenase from thermophilic, mesophilic and psychrophilic *Bacillus* spp. revealed a multitude of temperature-related amino acid substitutions, where the hydrophobic residues may be arranged from more thermophilic phenylalanine, valine, isoleucine and leucine to more mesophilic (or psychrophilic) methionine and alanine. In addition, the substitution from charged amino acids (glycine, asparagine, glutamine, serine and aspartate) in mesophilic and thermophilic chitinases to alanine at the equivalent CHI II positions 50, 59, 386 and 399 was also observed. This result indicated that the small hydrophobic alanine residue was preferred in cold-adapted enzymes to produce proteins with more flexibility and thus become more active at low environmental temperatures. An analysis of models from the cold-adapted archaea showed fewer charged residues as well as a strong tendency towards more hydrophobic residues and noncharged polar amino acids such as threonine in the solvent-accessible area [60]. Threonine appeared at positions 208, 311 and 363 in CHI II, while mesophilic and thermophilic chitinases were found to have other amino acid residues at equivalent locations, such as alanine, leucine, valine, tyrosine, tryptophan and phenylalanine.

Comparison of cold adaptations based on the structural characteristics of CHI II

A comparative structural analysis of CHI II with the experimentally determined structure of the mesophilic chitinase from *C. immitis*, 1D2K, was performed [37]. CHI II and the chitinase from *C. immitis* are both from the same group and have a similar TIM barrel fold and size; they also share the properties common to chitinolytic enzymes, but the enzymes are adapted to different temperature extremes. Therefore, these two molecules are an acceptable set of homologous enzymes for temperature adaptation studies. The structural parameters, such as the number of salt bridges and hydrogen bonds and the solvent interactions, including the hydrophobic, hydrophilic, positively and negatively charged accessible surface areas, were calculated and are shown in Table 4.

Salt bridges have been shown to be one of the main stabilising forces in protein structure. The disruption of a salt bridge can reduce the stability of a protein and vice versa [61]. Several comparative studies based on X-ray structure data have reported that the number of salt bridges is lower in cold-adapted enzymes [53]. Fewer salt bridges were identified in CHI II than in the mesophilic chitinase, 1D2K. The structural model of CHI II indicates that it has five arginine residues forming salt bridges, rather than the six in 1D2K. The lower total number of salt bridges, especially salt bridges formed by arginine residues, could explain the thermal instability of CHI II. Arginine residues are generally thought to enhance enzyme thermostability by facilitating a greater number of electrostatic interactions (up to two salt bridges and five H-bonds) through their guanidino group [62]. A previous study using X-ray structure data revealed that cold-adapted subtilisin has two salt bridges compared to the five or ten salt bridges in the corresponding mesophilic and thermophilic enzymes, respectively [54].

To further characterise the psychrophilicity of CHI II, the accessible surface areas of the hydrophobic, hydrophilic, positively charged and negatively charged residues were determined. The psychrophilic chitinase displayed an increased exposure of hydrophobic side chains to the solvent, whereas the mesophilic chitinase displayed an increase in the hydrophilic accessible surface area, including an increase in the charged accessible surface area. These differences lead to improved electrostatic interactions in the mesophilic chitinase that likely stabilise the enzyme at elevated temperatures. The surfaces of cold-adapted enzymes have a tendency to contain a higher proportion of hydrophobic (nonpolar) residues [53]. This has been demonstrated by the X-ray structures of adenylate kinases from the psychrophile *Bacillus globisporus* [63].

Therefore, the 40 % increase in the hydrophobic surface area of CHI II can be thought to increase the protein's structural flexibility under cold conditions, as was suggested by Tronelli et al. [4]. The hydrophobic surface residues destabilise the protein's structure due to the decreased entropy of the water molecules, which form cage-like structures around nonpolar residues. However, at low temperatures, the entropy gain is reduced due to the decreased mobility of the released water molecules [52]. This behaviour implies that cold-adapted enzymes may gain flexibility from and have a greater capacity to tolerate increased surface hydrophobicity [53]. The psychrophilic enzyme, CHI II, was found to have significantly fewer hydrogen bonds than mesophilic enzymes. Tronelli et al. [4] demonstrated the role of this type of electrostatic interaction when determining the greater stability of the quaternary structure in mesophilic and thermophilic proteins. However, at the moment, no satisfactory mechanistic explanation for the decrease in the number of hydrogen bonds has been proposed.

Conclusion

The development and analysis of a 3D model for the chitinase CHI II discovered several novel characteristics of the newly isolated cold-adapted protein from the psychrophilic yeast, *G. antarctica* PI12. The identification of another surface-exposed aromatic residue (Trp32) within the CHI II substrate-binding cleft is expected to have a profound effect on substrate binding. The existence of regions and amino acid residues that contribute to the local flexibility of the structure are in line with the capability of this enzyme to function in cold environments. The CHI II model developed may contribute to a better understanding of the structures and functions of other extremophilic proteins in nature.

Acknowledgments We would like to thank our colleagues Dr. Low Kheng Oon and Dr. Nurul Bahiyah Ahmad Khairudin from Faculty of Chemical Engineering, UTM for their valuable discussions. This work was supported by a research grant from the Molecular Biology & Genomic Initiative Program of the Malaysia Genome Institute (Project No. 07-05-16-MGI-GMB02). We would also like to express our appreciation to the Malaysia Antarctic Research Programme for their support.

References

1. Chen X-L, Xie B–B, Lu J-T, He H-L, Zhang Y (2007) A novel type of subtilase from the psychrotolerant bacterium *Pseudoalteromonas* sp. SM9913: catalytic and structural properties of deseasin MCP-01. Microbiology 153(7):2116–2125. doi:10.1099/mic.0.2007/006056-0
2. Kim S-Y, Hwang KY, Kim S-H, Sung H-C, Han YS, Cho Y (1999) Structural basis for cold adaptation. J Biol Chem 274(17):11761–11767
3. Russell RJM, Gerike U, Danson MJ, Hough DW, Taylor GL (1998) Structural adaptations of the cold-active citrate synthase from an Antarctic bacterium. Structure 6(3):351–361
4. Tronelli D, Maugini E, Bossa F, Pascarella S (2007) Structural adaptation to low temperatures—analysis of the subunit interface of oligomeric psychrophilic enzymes. FEBS J 274(17):4595–4608. doi:10.1111/j.1742-4658.2007.05988.x
5. Stefanidi E, Vorgias C (2008) Molecular analysis of the gene encoding a new chitinase from the marine psychrophilic bacterium *Moritella marina* and biochemical characterization of the recombinant enzyme. Extremophiles 12 (4):541–552-552. doi:10.1007/s00792-008-0155-9
6. Vaaje-Kolstad G, Houston DR, Rao FV, Peter MG, Synstad B, van Aalten DMF, Eijsink VGH (2004) Structure of the D142N mutant of the family 18 chitinase ChiB from *Serratia marcescens* and its complex with allosamidin. Biochimica et Biophysica Acta (BBA)—Proteins & Proteomics 1696 (1):103–111
7. Orikoshi H, Baba N, Nakayama S, Kashu H, Miyamoto K, Yasuda M, Inamori Y, Tsujibo H (2003) Molecular analysis of the gene encoding a novel cold-adapted chitinase (ChiB) from a Marine Bacterium, *Alteromonas* sp. Strain O-7. J Bacteriol 185(4):1153–1160. doi:10.1128/jb.185.4.1153-1160.2003
8. Nakamura T, Ishikawa M, Nakatani H, Oda A (2008) Characterization of cold-responsive extracellular chitinase in bromegrass cell cultures and its relationship to antifreeze activity. Plant Physiol 147(1):391–401. doi:10.1104/pp.106.081497
9. Fenice M, Selbmann L, Di Giambattista R, Federici F (1998) Chitinolytic activity at low temperature of an Antarctic strain (A3) of *Verticillium lecanii*. Res Microbiol 149(4):289–300
10. Facchiano AM, Stiuso P, Chiusano ML, Caraglia M, Giuberti G, Marra M, Abbruzzese A, Colonna G (2001) Homology modelling of the human eukaryotic initiation factor 5A (eIF-5A). Protein Eng 14(11):881–890. doi:10.1093/protein/14.11.881
11. Kelley LA, Sternberg MJE (2009) Protein structure prediction on the web: a case study using the Phyre server. Nat Protoc 4(3): 363–371
12. SÖding J, Biegert A, Lupas AN (2005) The HHpred interactive server for protein homology detection and structure prediction. Nucl Acids Res 33(2):W244–W248. doi:10.1093/nar/gki408
13. Jones DT (1999) GenTHREADER: an efficient and reliable protein fold recognition method for genomic sequences. J Mol Biol 287(4):797–815
14. Fornes O, Aragues R, Espadaler J, Marti-Renom MA, Sali A, Oliva B (2009) ModLink+: improving fold recognition by using protein–protein interactions. Bioinformatics 25(12):1506–1512. doi:10.1093/bioinformatics/btp238
15. Eswar N, Webb B, Marti-Renom M, Madhusudhan MS, Eramian D, Shen M-Y, Pieper U, Sali A (2007) Comparative protein structure modeling using MODELLER. Curr protoc protein sci 2(1):1–30
16. Marti-Renom MA, Stuart AC, Fiser A, Sanchez R, Melo F, Sali A (2000) Comparative protein structure modelling of genes and genomes. Annu Rev Biophys Biomol Struct 29(1):291–325. doi:10.1146/annurev.biophys.29.1.291
17. Schoonman MJL, Knegtel RMA, Grootenhuis PDJ (1998) Practical evaluation of comparative modelling and threading methods. Comput Chem 22(5):369–375
18. Ramli ANM, Mahadi NM, Rabu A, Murad AMA, Bakar FDA, Illias RM (2011) Molecular cloning, expression and biochemical characterisation of a cold-adapted novel recombinant chitinase from *Glaciozyma antarctica* PI12. Microb Cell Fact 10(1):1–13. doi:10.1186/1475-2859-10-94
19. Altschul SF, Gish W, Miller W, Myers EW, Lipman DJ (1990) Basic local alignment search tool. J Mol Biol 215(3):403–410
20. Altschul SF, Madden TL, Schaffer AA, Zhang J, Zhang Z, Miller W, Lipman DJ (1997) Gapped BLAST and PSI-BLAST: a new

generation of protein database search programs. Nucl Acids Res 25(17):3389–3402. doi:10.1093/nar/25.17.3389
21. Gough J, Karplus K, Hughey R, Chothia C (2001) Assignment of homology to genome sequences using a library of hidden Markov models that represent all proteins of known structure. J Mol Biol 313(4):903–919
22. Xu J, Zhang Y (2010) How significant is a protein structure similarity with TM-score = 0.5? Bioinformatics 26 (7):889–895. doi:10.1093/bioinformatics/btq066
23. Zhang Y, Skolnick J TM-align: a protein structure alignment algorithm based on the TM-score. Nucl Acids Res 33 (7): 2302–2309. doi:10.1093/nar/gki524
24. Guex N, Peitsch M (1997) SWISS-MODEL and the Swiss-Pdb viewer: an environment for comparative protein modeling. Electrophoresis 18(15):2714–2723
25. Laskowski RA, MacArthur MW, Moss DS, Thornton JM (1993) PROCHECK: a program to check the stereochemical quality of protein structures. J Appl Crystallogr 26(2):283–291. doi: 10.1107/s0021889892009944
26. Luthy R, Bowie JU, Eisenberg D (1992) Assessment of protein models with three-dimensional profiles. Nature 356(6364):83–85
27. Colovos C, Yeates TO (1993) Verification of protein structures: patterns of nonbonded atomic interactions. Protein Sci 2(9): 1511–1519. doi:10.1002/pro.5560020916
28. Wiederstein M, Sippl MJ (2007) ProSA-web: interactive web service for the recognition of errors in three-dimensional structures of proteins. Nucl Acids Res 35(2):W407–W410. doi: 10.1093/nar/gkm290
29. Darden T, York D, Pedersen L (1993) Particle mesh Ewald: an N [center-dot] log(N) method for Ewald sums in large systems. J Chem Phys 98(12):10089–10092
30. Hess B, Kutzner C, van der Spoel D, Lindahl E (2008) GROMACS 4: algorithms for highly efficient, load-balanced, and scalable molecular simulation. J Chem Theory Comput 4(3): 435–447
31. Costantini S, Colonna G, Facchiano AM (2008) ESBRI: a web server for evaluating salt bridges in proteins. Bioinformation 3(1):137–138
32. Wallon G, Lovett S, Magyar C, Svingor A, Szilagyi A, Zavodszky P, Ringe D, Petsko G (1997) Sequence and homology model of 3-isopropylmalate dehydrogenase from the psychrotrophic bacterium *Vibrio* sp. I5 suggest reasons for thermal instability. Protein Eng 10(6):665–672. doi:10.1093/protein/10.6.665
33. Delano WL (2002) The PyMOL molecular graphics system on World Wide Web http://www.pymol.org
34. Wahab H, Ahmad Khairudin N, Samian M, Najimudin N (2006) Sequence analysis and structure prediction of type II *Pseudomonas* sp. USM 4-55 PHA synthase and an insight into its catalytic mechanism. BMC Struct Biol 6 (1):23
35. Peng J, Xu J (2011) A multiple-template approach to protein threading. Proteins: structure, function, and bioinformatics:n/a-n/a. doi:10.1002/prot.23016
36. Chaitanya M, Babajan B, Anuradha C, Naveen M, Rajasekhar C, Madhusudana P, Kumar C (2010) Exploring the molecular basis for selective binding of *Mycobacterium tuberculosis* Asp kinase toward its natural substrates and feedback inhibitors: a docking and molecular dynamics study. J Mol Model 16(8):1357–1367. doi:10.1007/s00894-010-0653-4
37. Hollis T, Monzingo AF, Bortone K, Ernst S, Robertus JD, Cox R (2000) The X-ray structure of a chitinase from the pathogenic fungus *Coccidioides immitis*. Protein Sci 9(3):544–551. doi: 10.1110/ps.9.3.544
38. Matsumoto T, Nonaka T, Hashimoto M, Watanabe TYM (1999) Three-dimensional structure of the catalytic domain of chitinase Al *Bacillus circulans* WL-12 at a very high resolution. Proc Jpn Acad Ser B 75B(9):269–274
39. Terwisscha van Scheltinga AC, Hennig M, Dijkstra BW (1996) The 1.8 Å resolution structure of Hevamine, a plant chitinase/lysozyme, and analysis of the conserved sequence and structure motifs of glycosyl hydrolase family 18. J Mole Biol 262 (2):243–257
40. Hurtado-Guerrero R, van Aalten DMF (2007) Structure of *Saccharomyces cerevisiae* Chitinase 1 and screening-based discovery of potent inhibitors. Chem Biol 14(5):589–599
41. Watanabe T, Ariga Y, Sato U, Toratani T, Hashimoto M, Nikaidou N, Kezuka Y, Nonaka T, Sugiyama J (2003) Aromatic residues within the substrate-binding cleft of *Bacillus circulans* chitinase A1 are essential for hydrolysis of crystalline chitin. Biochem J 376(1):237–244. doi:10.1042/bj20030419
42. Perrakis A, Tews I, Dauter Z, Oppenheim AB, Chet I, Wilson KS, Vorgias CE (1994) Crystal structure of a bacterial chitinase at 2.3 Å resolution. Structure 2(12):1169–1180
43. Sun Y-J, Chang N-CA, Hung S-I, Chang AC, Chou C–C, Hsiao C-D (2001) The crystal structure of a novel mammalian lectin, Ym1, suggests a saccharide binding site. J Biol Chem 276(20): 17507–17514. doi:10.1074/jbc.M010416200
44. Li H, Greene LH (2010) Sequence and structural analysis of the chitinase insertion domain reveals two conserved motifs involved in chitin-binding. PLoS One 5(1):e8654
45. Palermo NY, Csontos J, Murphy RF, Lovas S (2008) Role of aromatic residues in stabilizing the secondary and tertiary structure of avian pancreatic polypeptide. Int J Quantum Chem 108(4):814–819. doi:10.1002/qua.21521
46. Aronson NN, Halloran BA, Alexyev MF, Amable L, Madura JD, Pasupulati L, Worth C, Van Roey P (2003) Family 18 chitinase-oligosaccharide substrate interaction: subsite preference and anomer selectivity of *Serratia marcescens* chitinase A. Biochem J 376(1):87–95. doi:10.1042/bj20030273
47. Zakariassen H, Aam BB, Horn SJ, Vårum KM, Sørlie M, Eijsink VGH (2009) Aromatic residues in the catalytic center of Chitinase A from *Serratia marcescens* affect processivity, enzyme activity, and biomass converting efficiency. J Biol Chem 284(16): 10610–10617. doi:10.1074/jbc.M900092200
48. Watanabe T, Kobori K, Miyashita K, Fujii T, Sakai H, Uchida M, Tanaka H (1993) Identification of glutamic acid 204 and aspartic acid 200 in chitinase A1 of *Bacillus circulans* WL-12 as essential residues for chitinase activity. J Biol Chem 268(25):18567–18572
49. Jarvis RA, Patrick EA (1973) Clustering using a similarity Measure based on shared near neighbors. Comput IEEE Transact on C-22 (11):1025–1034. doi:10.1109/t-c.1973.223640
50. Kundu S, Roy D (2009) Comparative structural studies of psychrophilic and mesophilic protein homologues by molecular dynamics simulation. J Mol Graph Model 27(8):871–880
51. Herning T, Yutani K, Inaka K, Kuroki R, Matsushima M, Kikuchi M (1992) Role of proline residues in human lysozyme stability: a scanning calorimetric study combined with x-ray structure analysis of proline mutants. Biochemistry 31(31):7077–7085. doi: 10.1021/bi00146a008
52. Kumar S, Nussinov R (2004) Different roles of electrostatics in heat and in cold: adaptation by citrate synthase. ChemBioChem 5(3):280–290. doi:10.1002/cbic.200300627
53. Siddiqui KS, Cavicchioli R (2006) Cold-adapted enzymes. Ann Rev Biochem 75(1):403–433. doi:10.1146/annurev.biochem.75.103004.142723
54. Davail S, Feller G, Narinx E, Gerday C (1994) Cold adaptation of proteins. Purification, characterization, and sequence of the heat-labile subtilisin from the antarctic psychrophile Bacillus TA41. J Biol Chem 269(26):17448–17453
55. Georlette D, Blaise V, Collins T, D'Amico S, Gratia E, Hoyoux A, Marx JC, Sonan G, Feller G, Gerday C (2004) Some like it

cold: biocatalysis at low temperatures. FEMS Microbiol Rev 28(1):25–42. doi:10.1016/j.femsre.2003.07.003
56. Paredes D, Watters K, Pitman D, Bystroff C, Dordick J Comparative void-volume analysis of psychrophilic and mesophilic enzymes: Structural bioinformatics of psychrophilic enzymes reveals sources of core flexibility. BMC Structural Biology 11(1):1–9. doi:10.1186/1472-6807-11-42
57. Alimenti C, Vallesi A, Pedrini B, Wüthrich K, Luporini P (2009) Molecular cold-adaptation: comparative analysis of two homologous families of psychrophilic and mesophilic signal proteins of the protozoan ciliate, Euplotes. IUBMB Life 61(8):838–845. doi:10.1002/iub.228
58. Galkin A, Kulakova L, Ashida H, Sawa Y, Esaki N (1999) Cold-adapted alanine dehydrogenases from two Antarctic bacterial strains: gene cloning, protein characterization, and comparison with mesophilic and thermophilic counterparts. Appl Environ Microbiol 65(9):4014–4020
59. Zuber H (1988) Temperature adaptation of lactate dehydrogenase Structural, functional and genetic aspects. Biophys Chem 29(1–2):171–179
60. Saunders NFW, Thomas T, Curmi PMG, Mattick JS, Kuczek E, Slade R, Davis J, Franzmann PD, Boone D, Rusterholtz K, Feldman R, Gates C, Bench S, Sowers K, Kadner K, Aerts A, Dehal P, Detter C, Glavina T, Lucas S, Richardson P, Larimer F, Hauser L, Land M, Cavicchioli R (2003) Mechanisms of Thermal Adaptation Revealed From the Genomes of the Antarctic *Archaea Methanogenium frigidum* and *Methanococcoides burtonii*. Genome Res 13(7):1580–1588. doi:10.1101/gr.1180903
61. Kumar S, Nussinov R (1999) Salt bridge stability in monomeric proteins. J Mol Biol 293(5):1241–1255
62. Feller G, Zekhnini Z, Lamotte-Brasseur J, Gerday C (1997) Enzymes from cold-adapted microorganisms. The class C β-lactamase from the antarctic psychrophile *Psychrobacter Immobilis* A5. Eur J Biochem 244 (1):186–191. doi:10.1111/j.1432-1033.1997.00186.x
63. Bae E, Phillips GN (2004) Structures and analysis of highly homologous psychrophilic, mesophilic, and thermophilic adenylate kinases. J Biol Chem 279(27):28202–28208. doi:10.1074/jbc.M401865200